Slip-trace-induced vicinal step destabilization

C. Coupeau,[*] O. Camara, M. Drouet, J. Durinck, J. Bonneville, J. Colin, and J. Grilhé

Institut P', Université de Poitiers, UPR 3346 CNRS, SP2MI-Téléport 2, F86962 Futuroscope-Chasseneuil Cedex, France
(Received 17 September 2015; revised manuscript received 4 November 2015; published 5 January 2016)

Gold single crystals were deformed by uniaxial compression tests with the help of an experimental apparatus that allows one to characterize *in situ*, by UHV scanning tunneling microscopy, the evolution of surface structures under stress. It is demonstrated that the slip traces resulting from the emergence of moving dislocations at the free surface highly modify the organization of the vicinal steps. A model based on energetic considerations is proposed and discussed to explain the observed phenomenon.

Understanding the atomic structures at the free surface of crystalline materials presents a main challenge in conferring new relevant physical properties to materials, for instance, in gold crystals, by controlling atomic reconstructions [1] or nanostructures and using them as templates for the self-organization of nanoparticules [2–7] or molecules [8–13]. Atomic surface structures are now currently investigated with the help of scanning probe microscopy. Crystallographic surfaces exhibit more or less extended terraces separated by steps at the atomic scale. The width of the terraces is controlled by the misorientation of the free surface with respect to the crystallographic structure of the specimen. The organization of the vicinal steps has been extensively studied in the past, for instance, the influence of temperature [14] and crystallographic indexes [15] on gold crystals and the effect of direct current on step bunching on silicon [16,17]. It has also been shown that an external applied stress may modify the reconstruction of the Si(001) surface [18]. On the other hand, stress may also involve plastic deformation, generally leading to slip traces at the free surfaces of strained crystalline materials. Slip traces are produced by the emergence of moving dislocations [19,20]; their fine analysis and characterization have proved to be of great interest for a better understanding of the elementary plastic mechanisms taking place in the bulk [21,22]. However, while sometimes suggested [23,24], to the best of our knowledge, experimental work regarding the interaction of slip traces with vicinal structures is lacking in the literature. In this Rapid Communication, we report experimental results obtained on strained gold single crystals. The evolution of the vicinal steps at increasing plastic strain is described and discussed in the frame of a model based on energetic considerations.

Gold single crystals were first prepared in a UHV environment by a sequence of ion sputtering (0.9 keV) and heating at approximately 850 K for 5–10 min. After a few preparation cycles, the (111) surface exhibits vicinal steps, as observed on Fig. 1(a). It is emphasized that the surface presents a partial vicinal character. However, it is shown that this partial vicinal character does not have any significant effect on the phenomenon described in the following (see Fig. S1 of the Supplemental Material [25]). The height of the atomic steps is experimentally found to be 0.24 nm, close to the theoretical

value of 0.235 nm. The usual herringbone pattern of the (111) terraces [20,26,27] is present but not visible in the scanning tunneling microscopy (STM) images displayed in Fig. 1. The limited quality results from experimental constraints to achieve *in situ* STM investigations under straining conditions, i.e., to capture the evolution of the steps (see Fig. S2 of the Supplemental Material [25] for *postmortem* images exhibiting the usual herringbone pattern with respect to the step structure). The samples were then mechanically strained using a home-made experimental apparatus allowing one to investigate *in situ*, by UHV atomic force microscopy (AFM)/STM, the evolution of sample surfaces under increasing stress/strain. As described in detail in Ref. [28], this setup successfully combines *in situ* mechanical compression tests under a UHV environment, together with atomic resolution near-field microscopy at variable temperatures, from 90 to 650 K, at strain rates ranging from 10^{-6} to 10^{-2} s^{-1}. The samples with a cross section of 2 mm × 2 mm and 6 mm in length were first deformed at 180 K by a uniaxial compression test along the [$\bar{1}$10] direction. From crystallographic considerations, slip traces are expected to lie along the [01$\bar{1}$] direction at ±60° from the compression axis. Slip traces result from the emergence of individual 1/2⟨110⟩ dislocations at the free surface of the sample. The height of a single trace corresponds to the Burgers vector $\vec{b}$ component perpendicular to the (111) surface [29]; theoretically, $h = \vec{b} \cdot \vec{n} = a/\sqrt{3}$, with $\vec{n}$ the normal to the free surface and a the lattice parameter, which for $a = 0.408$ nm leads to 0.235 nm. In Figs. 1(b) and 1(c) we present the resulting step structures at increasing plastic strains, $\varepsilon = 0.24\%$ and 0.29%, respectively. As expected, a few slip traces are evidenced lying at approximately 58° ± 3° from the compression axis. The slip traces intersect the vicinal steps, leading to a "checkered" pattern of different atomic levels. An intersecting point [denoted as X in Fig. 2(a)] between a vicinal step and a slip trace is surrounded by four terraces at different atomic levels, hereafter labeled (0), (1), and (2). It must be noted that two of them are at the same level (1). A white frame has been superimposed in Fig. 2(a) to highlight this characteristic surface feature.

Then, the temperature was raised up to 293 K in order to investigate the evolution of the "checkered" pattern with temperature. It took approximately half an hour to reach room temperature. Once the temperature has been stabilized at 293 K after approximately 1 h, the sample was investigated by STM. It is observed that the singularity (intersecting point X) has
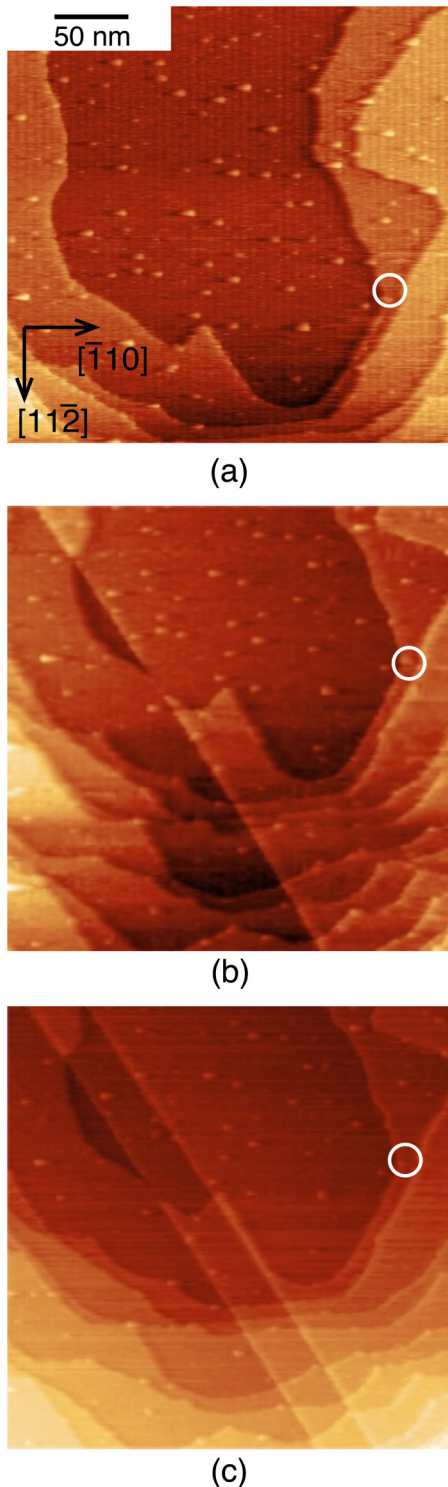
*christophe.coupeau@univ-poitiers.fr

(a)

(b)

(c)

FIG. 1. STM images of {111} surface of gold single crystals deformed along the [$\bar{1}$10] direction at $T = 180$ K for increasing macroscopic plastic strain: (a) $\varepsilon = 0.19\%$ (no visible slip trace), (b) $\varepsilon = 0.24\%$ (one visible slip trace), and (c) $\varepsilon = 0.29\%$ (two visible slip traces). The open white circle can be used as a marker to position each image with respect to the others.
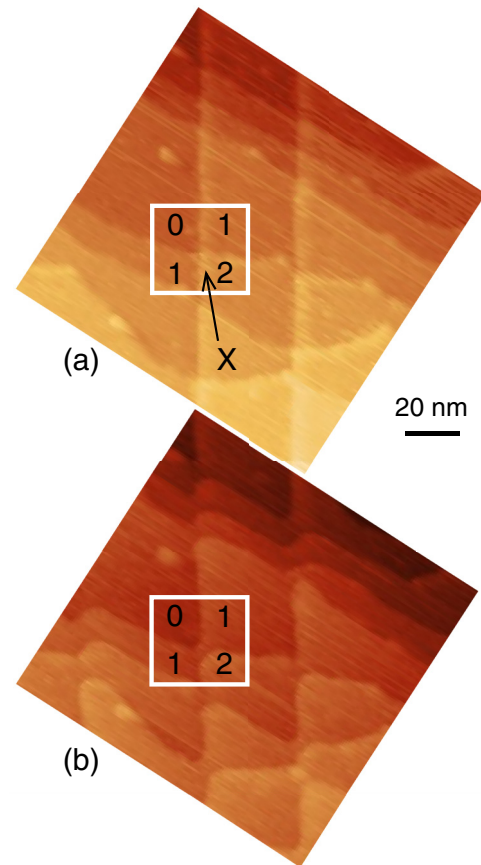

FIG. 2. STM images of the step structures under a stress of approximately 4 MPa (a) at $T = 180$ K and (b) after about 1 h at $T = 293$ K. A characteristic evolution is highlighted in the white frame. The intersection between a single-step slip trace and a vicinal step is denoted by X. The levels of the surrounding terraces are labeled (0), (1), and (2), respectively.

[see outside the white frame in Fig. 2(b)]. Moreover, the phenomenon has been observed on various gold specimens and at different deformation temperatures; in particular, direct deformation of the sample at 293 K leads to a similar final structure after less than 5 min. These experimental results highly suggest that the initial state is a kinetically limited structure, and the final state, an equilibrium one. The lower terrace at level (0) is "filled" near the intersecting point by gold atoms diffusing along the steps, while gold atoms diffused away from the intersecting point on the upper level [terrace at level (2)]. It leads to the coalescence of the two initial terraces at the same level (1), creating a "bridge" between them. It is assumed that the energy barrier to detach atoms from the kinks toward the terrace is high such that the atom density on the terraces is lower than the one on the steps [30]. As a consequence, the effect of terrace diffusion can be neglected compared to the one along the step lines. The scenario is schematically summarized in Fig. 3.

In our investigations only slip traces related to a single dislocation were observed. However, a slip trace may also result from the emergence of several dislocations that are moving in the same crystallographic plane, such as, for instance, in the case of a Frank-Read source [31]. Consequently,
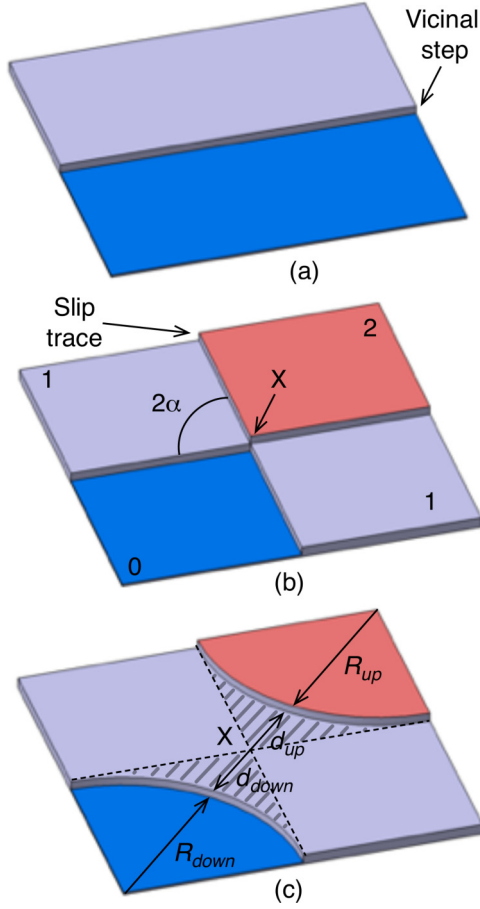
disappeared and is now replaced by two curved steps associated with three terraces at increasing levels only [Fig. 2(b)]. This phenomenon occurs on most of the intersecting points

FIG. 3. Schematic of the scenario. (a) Vicinal step. (b) Single trace resulting from the emergence of a single dislocation, which leads to a "checkered" structure. (c) Evolution of the "checkered" structure with the increase of temperature. 2α, d_i, and R_i correspond to the intersecting angle, the minimum distance between the crossing point X and the curved steps, and the radius of curvature of the curved steps, respectively (for $i = $ [up or down]).

the height of the resulting slip traces may be proportional to the atomic step unit. To take into account this latter possibility, a more general model that includes a multistep slip trace is first developed. In the following, the structure observed in Fig. 2(b) is defined by the angle 2α and the distances d_i, that are the angle between the slip trace and the vicinal step, and the shortest distances between the intersecting point X and the curved steps i, respectively [see Fig. 3(c)]. With this notation, 2α ranges from 0 to π and for $i = $ [up or down] depending on the upper or lower atomic levels. It is assumed that each curved portion can be described by a constant radius of curvature R_i. This assumption will be justified below. From a geometric point of view, 2α, d_i, and R_i are related by

$$\frac{d_i}{R_i} = \frac{1 - \cos\alpha}{\cos\alpha}. \tag{1}$$

The morphological aspect of various surface structures experimentally investigated by STM is summarized in Fig. 4. 2α is determined from the initial state (where the intersecting point is clearly defined), while d_i/R_i is extracted from the final state. The d_i/R_i ratio is presented in Fig. 4(a) as a function
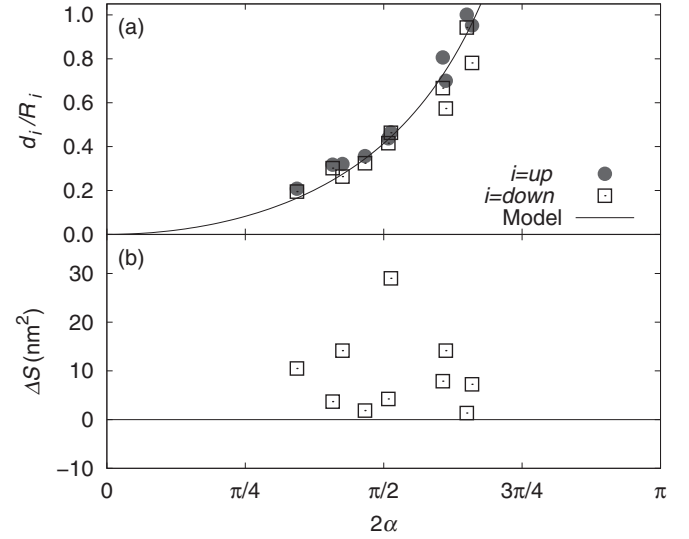

FIG. 4. Morphological aspect of the step structures. (a) d_i/R_i and (b) ΔS, vs 2α.

of 2α for $i = $ [up or down]. Whatever i, it is observed that d_i/R_i continuously increases with increasing 2α, in agreement with the expected behavior predicted by Eq. (1). This supports the hypothesis of constant radius of curvature for the final shape of each curved step. In Fig. 4(b), $\Delta S = S_{\text{up}} - S_{\text{down}}$ vs 2α is shown, where S_i are areas [dashed areas in Fig. 3(c)] defined by

$$S_i = R_i^2[\tan\alpha - \alpha]. \tag{2}$$

S_{up} and S_{down} characterize the number of outgoing and incoming gold atoms, respectively. Figure 4(b) gives evidence that all the observed structures are characterized by ΔS values greater than 0. This supports the idea of a diffusion phenomenon occurring preferentially along the steps instead of across the terraces for which ΔS should be zero. Moreover, it suggests that the diffusion process is more efficient on the upper step as compared to the lower one. This asymmetric behavior may be explained by the convex/concave aspect of the curvature radius and/or a local stress-induced effect.

Let us now consider a vicinal step sheared by a slip trace resulting from the emergence of n moving dislocations. In the case of two (or more) involved dislocations, it must be emphasized that a straight atomic step is still observable in the middle terrace, as schematically shown in Fig. 5. For the sake of simplicity, crystallographic effects have not been taken into account in the following. Likewise, the entropic and dipolar elastic energies of interaction between steps vary as $1/d^2$ [32,33]. As a consequence, both terms that first amplify the effect observed in the present work at short distances can be neglected with respect to the line energy term when d is of the order of a few nanometers. Finally, it is assumed that the surface energy is not modified by the morphological transformation. The energy balance from the surface structures described in Fig. 5(a) to those in Fig. 5(b) is consequently given by the following:

$$\text{for } n = 1: \quad \gamma_1 \sum_i 2\alpha R_i \leqslant 2\gamma_1 \sum_i R_i \tan\alpha, \tag{3}$$
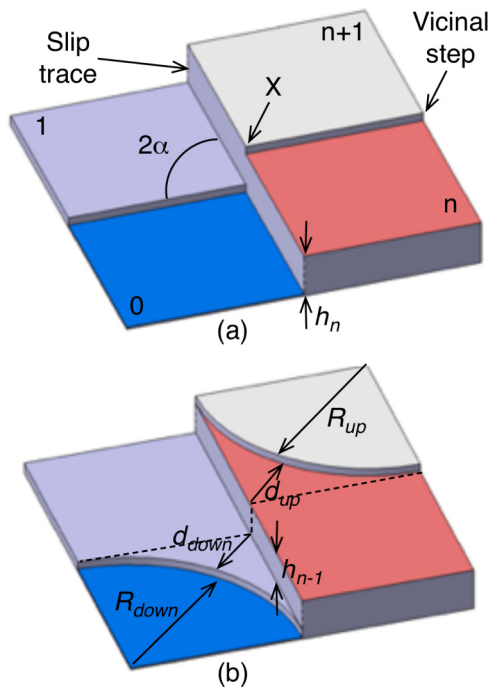
FIG. 5. Scenario of a slip trace resulting from n dislocations (a) before and (b) after the destabilization induced by atomic diffusion along the steps.

$$\text{for } n > 1: \quad \gamma_1 \sum_i 2\alpha R_i + \gamma_{n-1} \sum_i R_i \tan\alpha$$
$$\leqslant \gamma_1 \sum_i R_i \tan\alpha + \gamma_n \sum_i R_i \tan\alpha, \quad (4)$$

where γ_n, the line energy associated with a step with a height of n atomic levels. In the case where R_i is constant, as suggested in Fig. 4(a), Eq. (4) reduces to

$$\alpha \leqslant K_n \tan\alpha, \quad (5)$$

with K_n, a function of γ_n. It is found that $K_1 = 1$ and $K_n = (\gamma_1 - \gamma_{n-1} + \gamma_n)/(2\gamma_1)$ for $n > 1$.

For $n = 1$, Eq. (5) is always fulfilled since $2\alpha \in [0, \pi]$. That is, when a single-step slip trace intersects a vicinal step, curved steps are expected as the final state, whatever the intersecting angle, in agreement with the experimental results. It is worth noting that this phenomenon leads to blurred slip traces, or even makes them disappear from the free surface. Therefore, in such a case, it is not obvious to extract from the fine examinations of single-step slip traces the elementary plastic mechanisms taking place in the bulk.

For $n > 1$, two cases must be considered depending on K_n:

(i) For $K_n > 1$, Eq. (5) is still always valid whatever $2\alpha \in [0, \pi]$, so that curved steps should appear. This corresponds in particular to the case where $\gamma_n \geqslant n\gamma_1$, i.e., when the surface energy is greater than the associated line energy.

(ii) For $K_n < 1$, a critical angle which can be numerically calculated does exist below which the configurations with curved steps are no longer energetically favorable. The initial "checkered" nanostructure induced by the intersection of a multistep slip trace, i.e., with two (or more) dislocations, with a vicinal atomic step will be still observable at a low intersecting angle.

To conclude, in this Rapid Communication, we reported experimental results obtained on gold {111} strained single crystal surfaces. The investigations were performed using a home-made device allowing us to follow *in situ*, by UHV AFM/STM, the evolution of surface nanostructures under stress/strain. It is demonstrated that a single-step slip trace (i.e., related to the emergence of a single dislocation from the bulk) highly modifies the organization of the vicinal steps at free surfaces. The kinetics of the phenomenon is enhanced by increasing the temperature, which supports the idea of atomic diffusion involved in the process. A continuum model has been proposed to account for the experimental results. Whatever the intersecting angle between the slip trace and the vicinal step, the surface evolution is energetically favorable. The model also predicts the interactions between vicinal steps and slip traces resulting from several dislocations gliding in the same crystallographic plane (Frank-Read sources). In this case, a critical intersecting angle can be defined below which the configurations with curved steps are no longer energetically favorable. It depends on the line energies of steps of different height. Beyond the experimental results obtained on gold single crystals, the described phenomenon and the proposed model can be both extended to any materials for which the atomic surface diffusion is sufficiently active. It is believed that the presently reported phenomenon will be of particular interest to the materials science community and will give insight into how a surface can be structured at the nanometer scale, for instance, to be used as templates for conferring functional properties to materials.

[1] O. Schaff, A. K. Schmid, N. C. Bartelt, J. de la Figuera, and R. Q. Hwang, Mater. Sci. Eng., A **319-321**, 914 (2001).

[2] D. D. Chambliss, R. J. Wilson, and S. Chiang, Phys. Rev. Lett. **66**, 1721 (1991).

[3] B. Voigtländer, G. Meyer, and N. M. Amer, Phys. Rev. B **44**, 10354 (1991).

[4] E. I. Altman and R. J. Colton, Surf. Sci. **279**, 49 (1992).

[5] M. M. Biener, J. Biener, R. Schalek, and C. M. Friend, Surf. Sci. **594**, 221 (2005).

[6] N. A. Khan and C. Matranga, Surf. Sci. **602**, 932 (2008).

[7] R. Gaspari, C. A. Pignedoli, R. Fasel, M. Treier, and D. Passerone, Phys. Rev. B **82**, 041408 (2010).

[8] P. Fenter, A. Eberhardt, and P. Eisenberger, Science **266**, 1216 (1994).

[9] P. Wagner, M. Hegner, H.-J. Guentherodt, and G. Semenza, Langmuir **11**, 3867 (1995).

[10] M. Hara, H. Sasabe, and W. Knoll, Thin Solid Films **273**, 66 (1996).

[11] M. J. Comstock, J. Cho, A. Kirakosian, and M. F. Crommie, Phys. Rev. B **72**, 153414 (2005).

[12] P. Maksymovych, D. C. Sorescu, and J. T. Yates, Phys. Rev. Lett. **97**, 146103 (2006).

[13] E. Szőcs, L. Durrer, R. Luginbühl, N. Simic, A. S. Viana, L. M. Abrantes, R. Keese, and H. Siegenthaler, Surf. Sci. **600**, 43 (2006).

[14] M. Ondrejcek, M. Rajappan, W. Swiech, and C. Flynn, Surf. Sci. **574**, 111 (2005).

[15] G. Prévot, Y. Girard, V. Repain, S. Rousset, A. Coati, Y. Garreau, J. Paul, N. Mammen, and S. Narasimhan, Phys. Rev. B **81**, 075415 (2010).

[16] S. Yoshida, T. Sekiguchi, and K. M. Itoh, Appl. Phys. Lett. **87**, 031903 (2005).

[17] F. Leroy, D. Karashanova, M. Dufay, J.-M. Debierre, T. Frisch, J.-J. Métois, and P. Müller, Surf. Sci. **603**, 507 (2009).

[18] F. K. Men, W. E. Packard, and M. B. Webb, Phys. Rev. Lett. **61**, 2469 (1988).

[19] F. Foucher, C. Coupeau, J. Colin, A. Cimetière, and J. Grilhé, Phys. Rev. Lett. **97**, 096101 (2006).

[20] J. Engbæk, J. Schiøtz, B. Dahl-Madsen, and S. Horch, Phys. Rev. B **74**, 195434 (2006).

[21] O. Rodríguez de la Fuente, J. A. Zimmerman, M. A. González, J. de la Figuera, J. C. Hamilton, W. W. Pai, and J. M. Rojo, Phys. Rev. Lett. **88**, 036101 (2002).

[22] J. Christiansen, K. Morgenstern, J. Schiøtz, K. W. Jacobsen, K.-F. Braun, K.-H. Rieder, E. Lægsgaard, and F. Besenbacher, Phys. Rev. Lett. **88**, 206106 (2002).

[23] J. V. Barth, H. Brune, G. Ertl, and R. J. Behm, Phys. Rev. B **42**, 9307 (1990).

[24] H. Höche, J. P. Toennies, and R. Vollmer, Phys. Rev. B **50**, 679 (1994).

[25] See Supplemental Material at http://link.aps.org/supplemental/10.1103/PhysRevB.93.041405 where additional *postmortem* STM images are displayed.

[26] S. Narasimhan and D. Vanderbilt, Phys. Rev. Lett. **69**, 1564 (1992).

[27] V. Repain, J. M. Berroir, S. Rousset, and J. A. Lecoeur, Europhys. Lett. **47**, 435 (1999).

[28] Y. Nahas, F. Berneau, J. Bonneville, C. Coupeau, M. Drouet, B. Lamongie, M. Marteau, J. Michel, P. Tanguy, and C. Tromas, Rev. Sci. Instrum. **84**, 105117 (2013).

[29] C. Coupeau, J.-C. Girard, and J. Rabier, in *Dislocations in Solids*, edited by F. R. N. Nabarro and J. P. Hirth (Elsevier, Amsterdam, 2004), Vol. **12**, p. 273.

[30] H.-C. Jeong and E. D. Williams, Surf. Sci. Rep. **34**, 171 (1999).

[31] F. C. Frank and W. T. Read, Phys. Rev. **79**, 722 (1950).

[32] V. I. Marchenko and A. Ya Parshin, Zh. Eksp. Teor. Fiz. **79**, 257 (1980) [Sov. Phys. JETP **52**, 129 (1980)].

[33] C. Misbah, O. Pierre-Louis, and Y. Saito, Rev. Mod. Phys. **82**, 981 (2010).